

RESEARCH ARTICLE

Relationship of maternal cytomegalovirus-specific antibody responses and viral load to vertical transmission risk following primary maternal infection in a rhesus macaque model

Claire E. Otero^{1,2}, Richard Barfield³, Elizabeth Scheef⁴, Cody S. Nelson⁵, Nicole Rodgers⁶, Hsuan-Yuan Wang^{2,7}, Matilda J. Moström⁴, Tabitha D. Manuel⁴, Julian Sass⁸, Kimberli Schmidt⁹, Husam Taher¹⁰, Courtney Papan¹⁰, Lesli Sprehe⁴, Savannah Kendall⁴, Angel Davalos³, Peter A. Barry⁹, Klaus Früh¹⁰, Justin Pollara⁶, Daniel Malouli¹⁰, Cliburn Chan³, Amitinder Kaur⁴, Sallie R. Permar^{10,2*}

1 Department of Pathology, Duke University, Durham, North Carolina, United States of America, **2** Department of Pediatrics, Weill Cornell Medical College, New York, New York, United States of America, **3** Department of Biostatistics and Bioinformatics, Duke University, Durham, North Carolina, United States of America, **4** Tulane National Primate Research Center, Covington, Louisiana, United States of America, **5** Division of Allergy and Clinical Immunology, Department of Medicine, Brigham and Women's Hospital, Boston, Massachusetts, United States of America, **6** Duke Human Vaccine Institute & Department of Surgery, Duke University, Durham, North Carolina, United States of America, **7** Department of Immunology, Duke University, Durham, North Carolina, United States of America, **8** Department of Mathematics, North Carolina State University, Raleigh, North Carolina, United States of America, **9** Center for Immunology and Infectious Diseases, University of California, Davis, California, United States of America, **10** Vaccine and Gene Therapy Institute, Oregon Health & Science University, Beaverton, Oregon, United States of America

* sap4017@med.cornell.edu



OPEN ACCESS

Citation: Otero CE, Barfield R, Scheef E, Nelson CS, Rodgers N, Wang H-Y, et al. (2023) Relationship of maternal cytomegalovirus-specific antibody responses and viral load to vertical transmission risk following primary maternal infection in a rhesus macaque model. *PLoS Pathog* 19(10): e1011378. <https://doi.org/10.1371/journal.ppat.1011378>

Editor: Eain A. Murphy, State University of New York Upstate Medical University, UNITED STATES

Received: April 20, 2023

Accepted: September 29, 2023

Published: October 23, 2023

Peer Review History: PLOS recognizes the benefits of transparency in the peer review process; therefore, we enable the publication of all of the content of peer review and author responses alongside final, published articles. The editorial history of this article is available here: <https://doi.org/10.1371/journal.ppat.1011378>

Copyright: © 2023 Otero et al. This is an open access article distributed under the terms of the [Creative Commons Attribution License](https://creativecommons.org/licenses/by/4.0/), which permits unrestricted use, distribution, and reproduction in any medium, provided the original author and source are credited.

Data Availability Statement: All of the data used for figure generation and statistical analysis in this

Abstract

Cytomegalovirus (CMV) is the most common congenital infection and cause of birth defects worldwide. Primary CMV infection during pregnancy leads to a higher frequency of congenital CMV (cCMV) than maternal re-infection, suggesting that maternal immunity confers partial protection. However, poorly understood immune correlates of protection against placental transmission contributes to the current lack of an approved vaccine to prevent cCMV. In this study, we characterized the kinetics of maternal plasma rhesus CMV (RhCMV) viral load (VL) and RhCMV-specific antibody binding and functional responses in a group of 12 immunocompetent dams with acute, primary RhCMV infection. We defined cCMV transmission as RhCMV detection in amniotic fluid (AF) by qPCR. We then leveraged a large group of past and current primary RhCMV infection studies in late-first/early-second trimester RhCMV-seronegative rhesus macaque dams, including immunocompetent ($n = 15$), CD4+ T cell-depleted with ($n = 6$) and without ($n = 6$) RhCMV-specific polyclonal IgG infusion before infection to evaluate differences between RhCMV AF-positive and AF-negative dams. During the first 3 weeks after infection, the magnitude of RhCMV VL in maternal plasma was higher in AF-positive dams in the combined cohort, while RhCMV glycoprotein B (gB)- and pentamer-specific binding IgG responses were lower magnitude compared to AF-negative dams. However, these observed differences were driven by the CD4+ T cell-

manuscript can also be found at <https://github.com/ClaireEO/23-Humoral-and-viral-associates-of-congenital-RhCMV-risk>.

Funding: The primary funding for this work was NIH/NIAID 3P01AI129859 and NIH/NICHHD DP2HD075699 awarded to SRP. CEO conducted the majority of the work and was funded by NIH/NIAID 3P01AI129859-04S1 and NIH/NCI T32-CA009111. The Tulane National Primate Research Center (AK and team) is funded by NIH/NCRR (OD011104). The Oregon National Primate Research Center Molecular Virology Core (KF, DM, and team) is funded by NIH P51OD011092. The Biostatistics, Epidemiology and Research Design Methods Core (CC & RB) is funded by NIH/NCATS UL1TR002553. The funders had no role in study design, data collection and interpretation, decision to publish, or the preparation of this manuscript.

Competing interests: SRP provides individual consulting services to Moderna, Merck, Dynavax, Pfizer, GlaxoSmithKline (CMV vaccines) and HOOKIPA Biotech GmbH. She has also led sponsored research programs with Merck Vaccines and Moderna. Oregon Health Sciences University, KF and DM have a substantial financial interest in Vir Biotechnology, Inc. a company that may have a commercial interest in the results of this research and technology. KF and DM are co-inventors of several patents licensed to Vir Biotechnology. KF is also consultants to Vir Biotechnology, Inc. All potential conflicts of interest have been reviewed and managed by OHSU. These competing interests will not alter our adherence to PLOS policies on data and material sharing.

depleted dams, as there were no differences in plasma VL or antibody responses between immunocompetent AF-positive vs AF-negative dams. Overall, these results suggest that levels of neither maternal plasma viremia nor humoral responses are associated with cCMV following primary maternal infection in healthy individuals. We speculate that other factors related to innate immunity are more important in this context as antibody responses to acute infection likely develop too late to influence vertical transmission. Yet, pre-existing CMV glycoprotein-specific and neutralizing IgG may provide protection against cCMV following primary maternal CMV infection even in high-risk, immunocompromised settings.

Author summary

Cytomegalovirus (CMV) is the most common infectious cause of birth defects globally, but we still do not have licensed medical interventions to prevent vertical transmission of CMV. We utilized a non-human primate model of primary CMV infection during pregnancy to study virological and humoral factors that influence congenital infection. Unexpectedly, we found that the levels of virus in maternal plasma were not predictive of virus transmission to the amniotic fluid (AF) in immunocompetent dams. In contrast, CD4+ T cell depleted pregnant rhesus macaques with virus detected in AF had higher plasma viral loads than dams not showing placental transmission. Virus-specific antibody binding, neutralizing, and Fc-mediated antibody effector antibody responses were not different in immunocompetent animals with and without virus detectable in AF, but passively infused neutralizing antibodies and antibodies binding to key glycoproteins were higher in CD4+ T cell-depleted dams who did not transmit the virus compared to those that did. Our data suggests that the natural development of virus-specific antibody responses is too slow to prevent congenital transmission following maternal infection, highlighting the need for the development of vaccines that confer protective levels of immunity to CMV-naïve mothers that can prevent primary infection and/or congenital transmission to their infants during pregnancy.

Introduction

Cytomegalovirus (CMV) is the most common congenital infection and the leading non-genetic cause of hearing loss in pediatric populations [1,2]. Placental transmission following primary human CMV (HCMV) infection is much more common (30–40%) than after non-primary infection (3–4%), suggesting that the maternal immune system is effective in reducing the risk of vertical CMV transmission [3]. Furthermore, the biological factors contributing to or determining the likelihood of experiencing a congenital infection to the fetus in a subpopulation of CMV naïve women who contract a primary infection during pregnancy without having pre-existing CMV specific immunity remain poorly defined. Identification of immune responses that can naturally protect against congenital CMV (cCMV) would be enormously valuable for the rational design of an effective vaccine to prevent vertical CMV transmission.

The objective of this study was to identify maternal humoral immune responses associated with vertical CMV transmission in the high-risk setting of primary maternal infection, as a strategy to guide vaccine development. The study of primary CMV infection faces several logistical hurdles. First, primary CMV infection is difficult to detect in humans because CMV infection is typically asymptomatic or exceedingly mild in healthy individuals, including

during pregnancy [4]. This diagnostic dilemma makes human studies of early immune responses to infection challenging. Unfortunately, HCMV cannot be used to infect any animal model commonly used in the laboratory to study virus pathogenesis as all examined CMV species exhibit a high degree of species-specificity and can hence only productively replicate in the host species they have co-evolved with [5,6]. Moreover, not all animal CMVs cross the placenta, which may be a result of differences in placental biology or viral characteristics, further limiting animal models for the study of cCMV and placental CMV transmission [7,8]. Non-human primates (NHPs) bear the closest resemblance to humans in terms of anatomy and physiology of pregnancy, and immune responses to viral infection [9,10,11,12]. Furthermore, the continuous immunological arms race between CMVs and their host species has resulted in an ongoing, mutual virus/host co-adaptation reflected in the congruence of NHP and NHP-CMV phylogenetic trees and strict species specificity [13]. Hence, NHP CMVs represent the closest relatives to HCMV as they share the most recent common ancestor, and conservation of coding ORFs and gene families, viral immune evasion strategies and viral pathogenesis has been demonstrated [14]. Thus, we have developed a rhesus macaque model of primary, maternal CMV infection during the early stages of pregnancy, at the intersection of the first and second trimesters of gestation. In this model, congenital transmission occurs in a fraction of immunocompetent pregnant animals (dams) and universally in CD4+ T cell depleted dams without additional intervention [15], which has proven useful in defining the immunological and virological determinants of cCMV transmission [16].

We hypothesized that high magnitude maternal viremia is associated with vertical RhCMV transmission, particularly in this setting of primary maternal infection where no pre-existing immunity exists. We reasoned that increased virus circulation in the maternal blood should result in a greater viral load (VL) at the maternal-fetal interface, increasing the likelihood of placental infection and congenital transmission. This idea has recently been supported by mathematical modeling of vertical CMV transmission [17]. Furthermore, we hypothesized that maternal virus-specific functional antibody responses such as neutralization, antibody dependent cellular cytotoxicity (ADCC), and antibody dependent cellular phagocytosis (ADCP) are important for controlling viral replication and preventing vertical transmission, as cell-to-cell spread is a key mechanism for CMV dissemination [18], meaning that antibody functions that target both cell-free and cell-associated virus may be needed for adequate control.

We leveraged multiple RhCMV-seronegative, pregnant NHP groups that were challenged with RhCMV at the end of the first/early second trimester of pregnancy from prior and current studies modeling vertical CMV transmission: a cohort of 15 total immunocompetent dams (3 dams from a historical study and 12 dams from a current study), 6 dams that received a single dose of CD4 T cell-depleting antibody 1 week prior to infection, and 6 total dams that were CD4+ T cell depleted (CD4-depleted) 1 week prior to infection and received a polyclonal RhCMV-specific IgG infusion just prior to infection to model pre-existing antibody [15,16]. We began by characterizing the antibody responses in a novel cohort of 12 immunocompetent, acutely RhCMV-infected dams, including ADCP and ADCC functions, which had not been previously measured in the context of RhCMV infection. Many of these responses have been previously reported for the historical cohorts, and available plasma samples from these studies were re-analyzed for recently developed functional antibody assays. Subsequent analysis of these responses and maternal VL revealed no significant differences in the magnitude of these variables in immunocompetent dams that did or did not have detectable virus in amniotic fluid (AF), but RhCMV glycoprotein-specific binding responses and neutralizing antibody responses were higher magnitude in CD4-depleted animals that received passive IgG infusion and did not have viral DNA detectable in AF compared to those that did.

Results

RhCMV vertical transmission confirmed in 5/12 immunocompetent dams following primary RhCMV infection during pregnancy by detection of virus in AF

We challenged 12 RhCMV-seronegative rhesus dams via intravenous injection of both 1.0×10^6 pfu of the epithelial-tropic, low passage isolate UCD52 RhCMV strain and 1.0×10^6 pfu of a bacterial artificial chromosome (BAC)-derived, clonal full-length (FL) RhCMV fully repaired for genes missing from the parental fibroblast-adapted 68-1 strain [19]. We monitored VL of maternal plasma and AF following RhCMV infection using qPCR detection of viral DNA targeting the noncoding exon 1 region of the RhCMV IE gene [20] or the gB gene (*UL55*). Plasma VL peaked 1–2 weeks post infection in all dams, and many had detectable VL through 14 weeks post infection (Fig 1B). Five of the twelve dams in this cohort had CMV DNA detectable by qPCR in the AF collected weekly between 2–12 weeks after infection, confirming vertical transmission (AF-positive). AF virus was detected within 4 weeks post infection in three dams

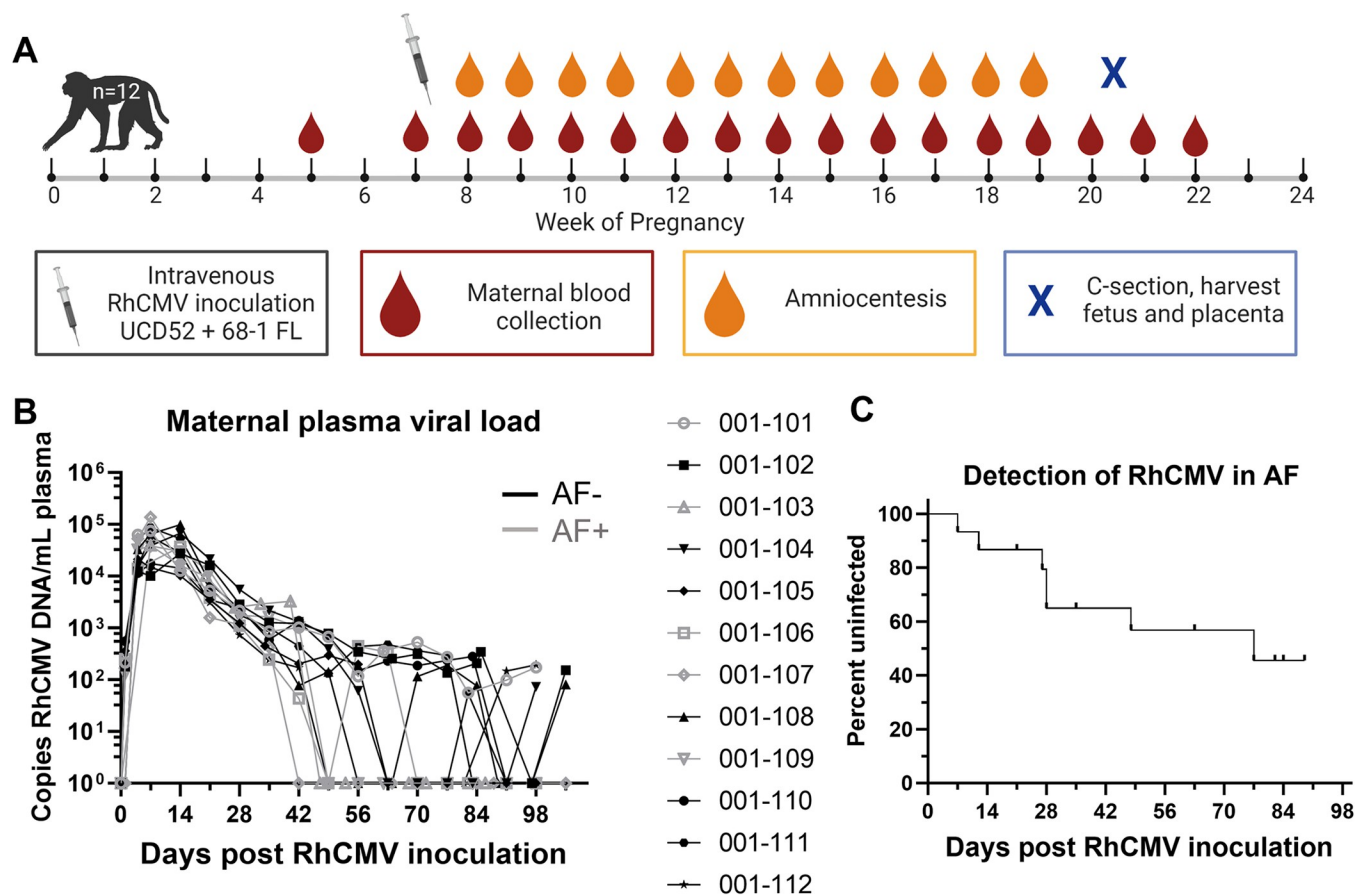


Fig 1. Plasma VL and vertical transmission events following primary maternal RhCMV infection in immunocompetent dams (n = 12). (A) The study schedule for a new cohort of 12 RhCMV seronegative, pregnant rhesus macaques receiving intravenous inoculation of 1×10^6 pfu of two RhCMV strains (clinical isolate UCD52 and cloned full length, FL, 68-1 viral variants) in late first/early second trimester, followed by weekly blood draws and amniocentesis until hysterotomy near term at 20–22 weeks gestation, prior to fetal viability. A pre-infection blood draw was collected between 1–4 weeks before infection. (B) Maternal plasma VL kinetics measured by qPCR against either RhCMV gB (*UL55*) or the noncoding exon 1 region of the RhCMV IE gene for RhCMV-positive amniotic fluid (AF-positive, n = 5) and AF-negative (n = 7) dams. Data shown as the mean value of 6 or more technical replicates for each sample. (C) Survival curve showing the timing of detection of vertical transmission, defined as amniotic fluid RhCMV qPCR result above the limit of detection in 2 or more of 12 technical replicates. Vertical transmission was confirmed in 5/12 dams by this definition. Schematic created using [Biorender.com](https://biorender.com).

<https://doi.org/10.1371/journal.ppat.1011378.g001>

and after 6 weeks post infection in the remaining two AF-positive dams (Fig 1C). Importantly, the kinetics of the plasma VL was similar in AF-positive vs AF-negative dams.

RhCMV-specific antibody binding kinetics following primary RhCMV infection during pregnancy

Plasma RhCMV-specific IgM responses were detectable at low levels by 2 weeks post infection and remained elevated throughout the pregnancy (Fig 2A). IgG binding to whole RhCMV virions and key envelope glycoproteins, glycoprotein B (gB) and the pentameric complex (PC), shared similar kinetics, with detectable responses by 2 weeks post infection in most animals, with a sharp increase in antibody titers between 2–4 weeks post infection followed by a plateau or a more gradual increase in antibody levels throughout the remainder of the pregnancy (Fig 2B–2E). Notably, we measured gB-specific IgG binding to both soluble ectodomain via enzyme-linked immunosorbent assay (ELISA) and cell-associated gB via a transfected cell binding flow cytometry-based assay, and each demonstrated similar kinetics (Fig 2C and 2D). Overall, these responses are largely consistent with the expected binding antibody responses during the acute phase of infection in humans [21].

RhCMV-specific antibody effector function kinetics following primary RhCMV infection during pregnancy

Similar to the kinetics of the RhCMV-specific IgG binding responses, RhCMV-neutralizing responses in both fibroblast and epithelial cells developed within 3 weeks post infection, reached an inflection point by 6 weeks post infection, and then gradually increased over the remainder of pregnancy (Fig 3A and 3B). In contrast, non-neutralizing Fc-mediated antibody effector responses, ADCP (antibody-mediated uptake by THP-1 monocytes) and ADCC

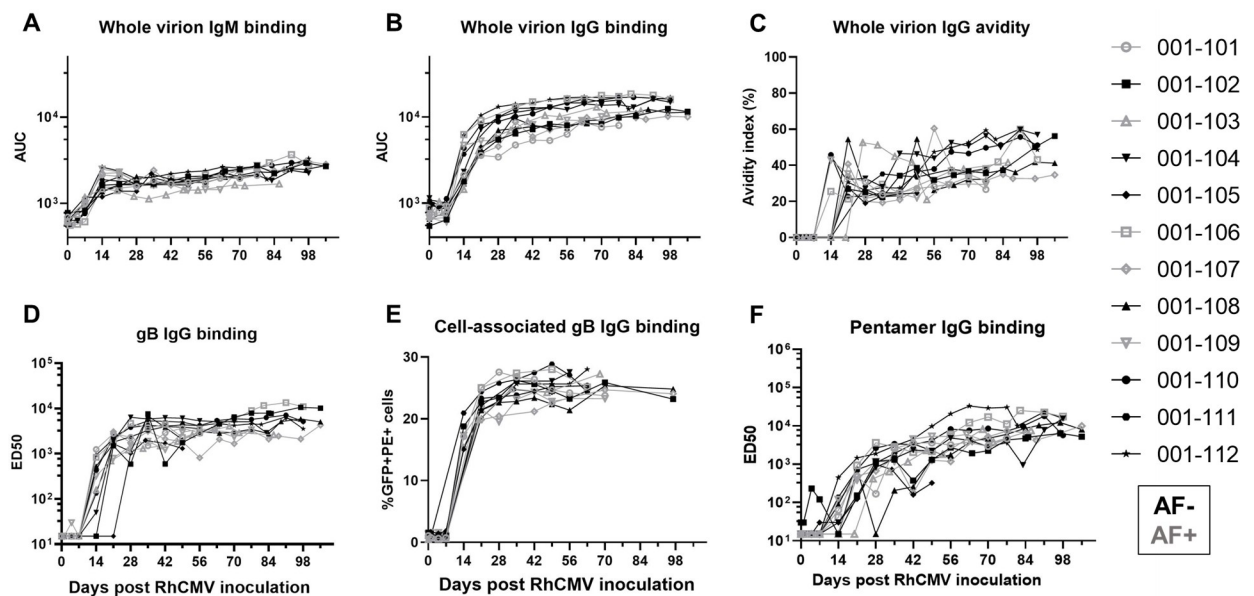


Fig 2. Plasma RhCMV-specific IgM and IgG binding responses following acute RhCMV infection during pregnancy. In a novel cohort of 12 RhCMV seronegative, immunocompetent dams primarily infected with RhCMV at the end of first/early second trimester of pregnancy, we measured the following RhCMV-specific antibody binding responses longitudinally: (A) IgM binding to whole UCD52 RhCMV virions, (B) IgG binding to whole UCD52 virions, (C) avidity of IgG binding to whole UCD52 virions, (D) IgG binding to the ectodomain of UCD52 gB, (E) IgG binding to cell-associated UCD52 gB, and (F) IgG binding to soluble PC. AF-positive dams are shown in grey, and AF-negative dams are shown in black. Data shown as the mean of technical duplicates.

<https://doi.org/10.1371/journal.ppat.1011378.g002>

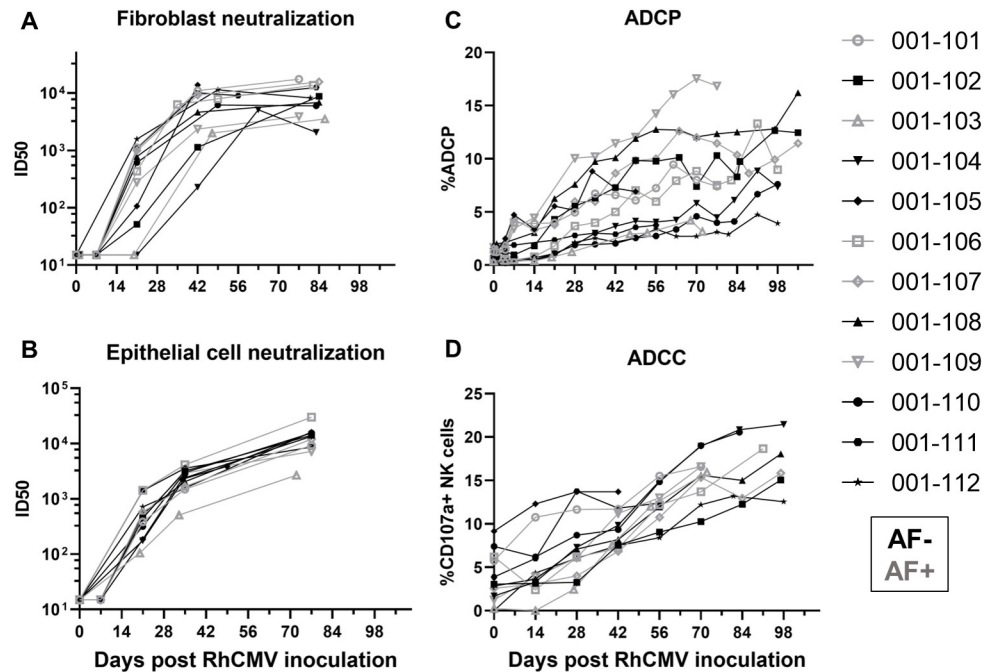


Fig 3. The kinetics of functional RhCMV-specific antibody responses in plasma during acute maternal infection. We measured functional antibody responses longitudinally in a novel cohort of 12 immunocompetent dams with primary RhCMV infection during pregnancy. (A) Neutralization of FL RhCMV on telomerized rhesus fibroblasts (TeloRFs), (B) neutralization of UCD52 RhCMV on monkey kidney epithelial cells, (C) monocyte-mediated antibody dependent cellular phagocytosis against free UCD52 RhCMV, (D) NK cell degranulation, a component of cell-mediated antibody dependent cellular cytotoxicity against UCD52-infected TeloRFs. Data shown as the mean of technical duplicates.

<https://doi.org/10.1371/journal.ppat.1011378.g003>

(measured as antibody-mediated NK cell degranulation) [22], generally developed more gradually over the course of the infection and never reached a clear peak during the study period (Fig 3C and 3D). Importantly, the kinetics of all antibody responses were similar in AF-positive and AF-negative dams (Figs 2 and 3).

Inclusion of historical CD4-depleted and IgG-infused groups introduces perturbations of measured responses

For further analysis, we incorporated data from past studies of rhesus dams with primary RhCMV infection in late first / early second trimester [15,16]. The timing of maternal infection, administration of RhCMV, and total inoculum dose are similar among all of these groups, but the virus strains and immunologic manipulations differ somewhat among the groups (Fig 4). Most animals from historical studies were infected with a cocktail of three RhCMV strains including low-passage epithelial-tropic isolates UCD52 and UCD59 along with the laboratory-adapted 180.92, which is a mixed virus with the dominant sequenced variant having a truncated UL/b' region that still retains an intact UL128-UL131 locus [20]. One animal (274-98) from prior studies received only 180.92. Notably, all viruses included in the inoculums express the PC. As reported in these previous studies, CD4-depletion results in higher maternal plasma VL, consistent vertical RhCMV transmission, and a high rate of fetal loss compared to immunocompetent dams [15]. However, infusion of IgG purified from seropositive RMs with robust anti-RhCMV neutralizing responses prior to infection leads to a reduction in maternal plasma VL and demonstrated protection in this extremely high risk setting of CD4-depletion [16]. We chose to include animals from these previous studies to bolster the total sample size and

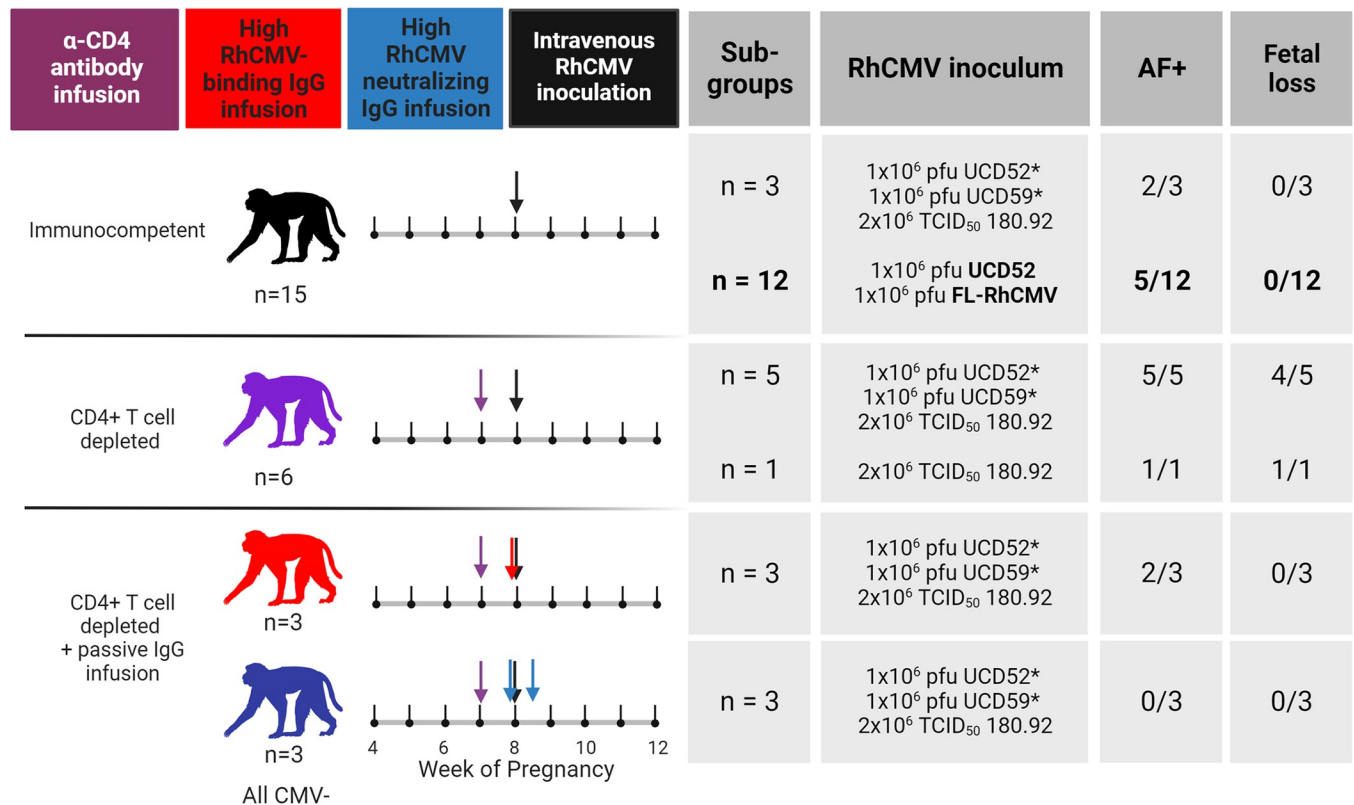


Fig 4. Combination of RhCMV seronegative, pregnant rhesus macaque cohorts. Treatment schedules for each of the rhesus macaque cohorts included in the combined analysis. A new group of 12 immunocompetent dams is highlighted in bold, and all other groups are from historical studies completed between 2013–2016 [15,16]. All dams were infected by intravenous inoculation of the RhCMV strains listed with 1x10⁶ pfu for each UCD52, UCD59, (*previously reported as 1x10⁶ TCID₅₀ [15,16], rounded from 1.4x10⁶ TCID₅₀) and FL RhCMV, and 2x10⁶ TCID₅₀ for 180.92 (for a total of 2–3x10⁶ total infectious virions) at week 7–9 of gestation. A total of 15 immunocompetent dams (black) included 3 dams from a previous study in which animals received a 1:1:2 combination of low passage isolates UCD52 and UCD59 and lab adapted strain 180.92 as well as 12 dams inoculated with a 1:1 combination of UCD52 and BAC-derived full length (FL) RhCMV. A total of 6 dams received a 50 mg/kg dose of recombinant rhesus anti-CD4+ T-cell-depleting antibody 1 week prior to infection. Five of these dams were infected with 1:1:2 UCD52, UCD59, and 180.92, and the remaining dam was infected with 180.92 alone. Six additional animals received CD4-depleting antibody 1 week before infection and passive infusion of a polyclonal RhCMV-positive IgG preparation before infection with 1:1:2 UCD52, UCD59, and 180.92. IgG for passive infusion was purified from RhCMV-seropositive plasma donors screened for high RhCMV binding (red) or high RhCMV neutralization on epithelial cells (blue). The high RhCMV binding IgG infusion was given at a single 100 mg/kg dose 1 hour before infection, and the high RhCMV neutralizing IgG infusion was given in a two-dose, optimized regimen with the initial 150 mg/kg dose 1 hour prior to infection and the second 100 mg/kg dose 3 days post infection. Of the immunocompetent dams, 7/15 had detectable RhCMV DNA in amniotic fluid. All 6 of the CD4-depleted dams were AF-positive, and 5 experienced spontaneous abortion. Two of the dams receiving the high RhCMV binding IgG infusion and none of the dams receiving the high RhCMV neutralizing IgG infusion were AF-positive. Figure created using [Biorender.com](https://www.biorender.com).

<https://doi.org/10.1371/journal.ppat.1011378.g004>

introduce the following perturbations to the measured responses: 1) maternal plasma VL was higher in CD4-depleted animals and lower in CD4-depleted animals receiving a potentially-RhCMV neutralizing IgG infusion, 2) humoral responses were generally delayed in CD4-depleted, acutely-infected dams, and 3) dams receiving passive IgG infusion before infection had high levels of RhCMV-specific IgG in the first week of infection (Fig 5). With the understanding that treatment group is a potential confounding factor, we performed subgroup analyses for our primary analysis of pairwise comparisons between AF-positive and AF-negative dams.

The magnitude of the plasma VL is not significantly different between AF-positive versus AF-negative immunocompetent dams

To distill each virologic and immunologic variable for comparison across AF-positive and AF-negative dams, we calculated the area-under-the-curve (AUC) for the first three weeks post

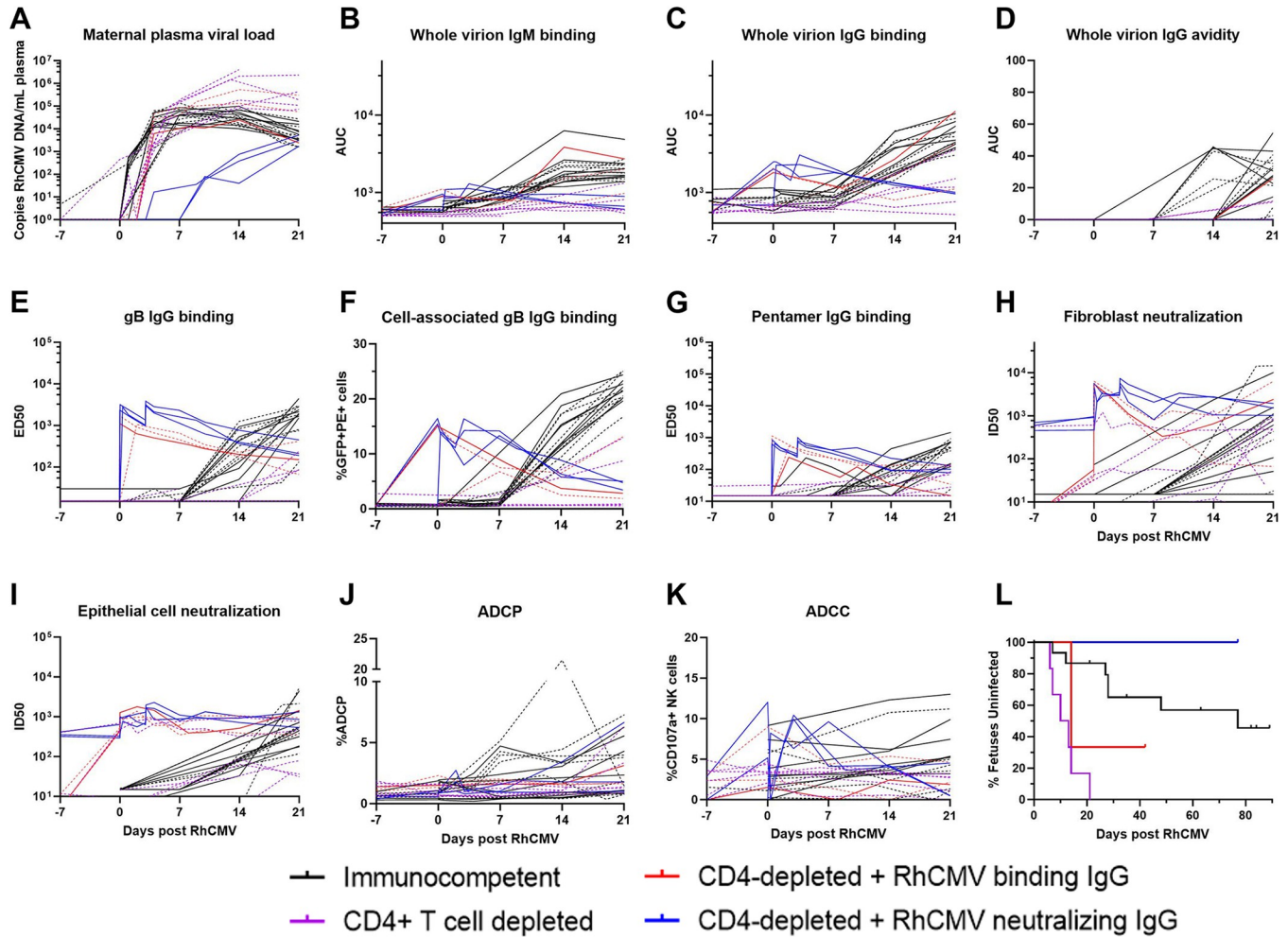


Fig 5. Kinetics of plasma VL and RhCMV-specific antibody responses for all treatment groups through 3 weeks post RhCMV infection. (A) Maternal plasma VL measured by qPCR for the UL55 or IE genes; (B) IgM and (C) IgG binding to whole UCD52 RhCMV virions; (D) avidity of IgG binding against whole UCD52 virions; IgG binding to (E) PC, (F) soluble gB ectodomain by ELISA, and (G) cell-associated gB via transfected cell binding assay; antibody mediated RhCMV neutralization on (H) fibroblasts and (I) epithelial cells; (J) ADCP; and (K) ADCC; (L) Survival curves showing detection of RhCMV in amniotic fluid. Treatment groups are represented by the color of each line. Solid lines represent AF-negative dams, and dashed lines represent AF-positive dams. Previously published data for historical studies was used for soluble gB- and PC-binding IgG responses and fibroblast and epithelial cell neutralization [15,16], and available samples from those studies were utilized for measurement of remaining assays.

<https://doi.org/10.1371/journal.ppat.1011378.g005>

infection, which is the time period when vertical RhCMV transmission most often occurred and each measured response developed in this model (Fig 5) [15,16]. The maternal plasma VL was not significantly different between AF-positive vs AF-negative dams in the immunocompetent group (Wilcoxon $p_{unadj} = 0.69$, $p_{FDR} = 0.89$, Table 1 and Fig 6). In stark contrast, plasma VL was higher in AF-positive dams compared to AF-negative dams in the CD4-depleted groups ($p_{unadj} = 0.004$, $p_{FDR} = 0.044$, Table 1 and Fig 7), driving a significant difference in the maternal plasma VLs in the combined group including both all treatment groups ($p_{unadj} = 0.0013$, $p_{FDR} = 0.0014$, Table 1). However, the differences in plasma VL in CD4-depleted dams is largely confounded by the treatment group, as all four AF-negative CD4-depleted animals received passive IgG infusion before infection and all six of the CD4-depleted dams without pre-existing antibody were AF-positive (Fig 4). Thus, pre-existing CMV-targeting IgG antibodies may have contributed directly to the reduction in plasma VL and the absence of vertical CMV transmission.

Table 1. Univariate analysis comparing AF-positive versus AF-negative dams within subgroups.

Response	Immunocompetent (n = 15)		CD4-depleted (n = 12)		Combined cohort (n = 27)	
	Effect size	P _{unadjusted} (P _{FDR})	Effect size	P _{unadjusted} (P _{FDR})	Effect size	P _{unadjusted} (P _{FDR})
Maternal plasma viral load	0.120	0.694 (0.885)	0.784	0.00404 (0.0444)	0.579	0.00128 (0.0141)
Cell-associated gB binding	0.239	0.397 (0.885)	0.686	0.0162 (0.0444)	0.462	0.0148 (0.0814)
PC IgG binding (ELISA)	0.179	0.536 (0.885)	0.637	0.0283 (0.0519)	0.392	0.0407 (0.149)
gB IgG binding (ELISA)	0.030	0.955 (0.955)	0.688	0.0162 (0.0444)	0.361	0.0601 (0.164)
Whole virion IgG binding	0.209	0.463 (0.885)	0.490	0.109 (0.150)	0.345	0.0743 (0.164)
Neutralization on epithelial cells	0.120	0.694 (0.885)	0.686	0.0162 (0.0444)	0.308	0.114 (0.185)
ADCC	0.254	0.351 (0.885)	0.392	0.214 (0.236)	0.304	0.118 (0.185)
Neutralization on fibroblasts	0.075	0.805 (0.885)	0.637	0.0283 (0.0519)	0.292	0.135 (0.185)
Whole virion IgM binding	0.149	0.613 (0.885)	0.539	0.0727 (0.114)	0.178	0.376 (0.460)
Whole virion IgG avidity	0.090	0.779 (0.885)	0.064	0.830 (0.830)	0.133	0.518 (0.570)
ADCP	0.269	0.336 (0.885)	0.441	0.154 (0.188)	0.032	0.886 (0.886)

P-values show exact results from Wilcoxon Rank Sum Tests as unadjusted p-value (FDR p-value). **Bold** indicates P-value <0.05 and FDR p-value <0.2. Abbreviations: Amniotic fluid (AF), False Discovery Rate corrected (FDR); immunoglobulin M (IgM), immunoglobulin G (IgG), glycoprotein B (gB), enzyme-linked immunosorbent assay (ELISA), pentameric complex (PC), antibody dependent cellular phagocytosis (ADCP), antibody dependent cellular cytotoxicity (ADCC).

<https://doi.org/10.1371/journal.ppat.1011378.t001>

Humoral immune responses are not statistically significantly different between AF-positive and AF-negative immunocompetent, acutely RhCMV-infected dams, yet plasma cell-associated gB and PC-specific IgG responses were higher magnitude in AF-negative dams from the entire cohort

As observed for maternal plasma VL, none of the measured RhCMV-specific binding or functional antibody responses were statistically different in AF-positive versus AF-negative immunocompetent dams (Table 1 and Fig 6), including CMV-specific IgG avidity, which was previously reported to be associated with vertical transmission risk in humans [23]. In comparing RhCMV-specific humoral responses across the entire dam cohort, only two responses were statistically associated with transmission status: plasma IgG binding to cell-associated gB ($p_{unadj} = 0.015$, $p_{FDR} = 0.081$) and soluble PC ($p_{unadj} = 0.041$, $p_{FDR} = 0.15$). Within the CD4-depleted groups, plasma RhCMV glycoprotein-binding IgG responses and neutralization in both fibroblasts and epithelial cells were statistically higher in AF-negative compared to AF-positive dams by unadjusted Wilcoxon Rank Sum tests (Table 1 and Fig 7). Thus, all differences in the RhCMV-specific IgG responses in AF-positive vs AF-negative dams were driven by the CD4-depleted dam groups.

Plasma RhCMV-specific antibody responses are indirectly related to plasma VL

Using Spearman's rank correlations, we found that all of the measured RhCMV-specific antibody responses demonstrated weak negative associations with maternal plasma VL across the

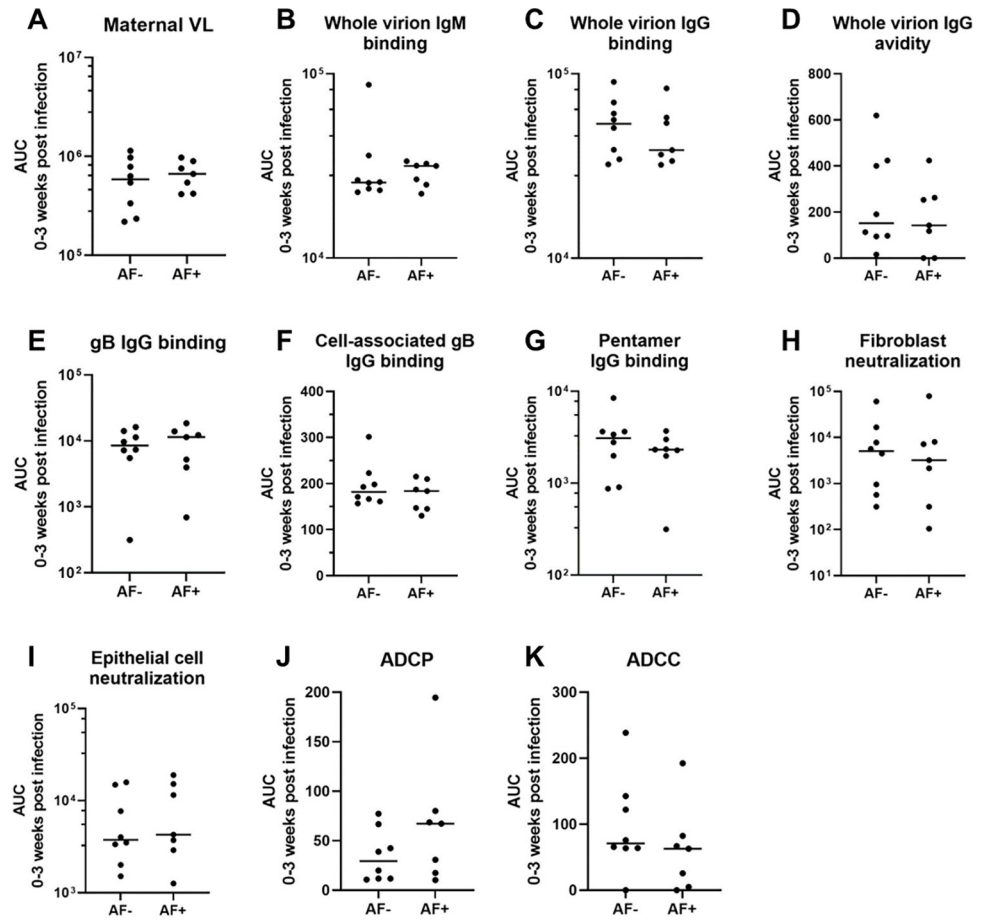


Fig 6. Univariate comparison of maternal VL and humoral responses by vertical transmission status in immunocompetent dams. The area-under-the-curve (AUC) of each response over 0–3 weeks post RhCMV infection was used to distill the magnitude and kinetics of each response into a single value in a critical window for vertical transmission. Amniotic fluid (AF) was assessed for RhCMV DNA by qPCR and a positive result (AF-positive) was defined by 2 or more of 12 replicates with detectable amplification between 2 and 12 weeks after maternal infection. Pairwise comparisons between AF-positive and AF-negative dams were performed using Wilcoxon Rank Sum Tests (Table 1). VL: viral load; ADCP: antibody dependent cellular phagocytosis; ADCC: antibody dependent cellular cytotoxicity.

<https://doi.org/10.1371/journal.ppat.1011378.g006>

entire cohort (Fig 8A). Further, we found moderately strong positive associations between IgG and IgM binding to whole UCD52 virions ($r = 0.74$, 95% CI: 0.44, 0.91), soluble gB and PC IgG binding ($r = 0.83$, 95% CI: 0.64, 0.91), and between fibroblast and epithelial cell neutralization responses ($r = 0.62$, 95% CI: 0.23, 0.86). There were also moderate positive associations between the glycoprotein-specific IgG binding and neutralization responses (Fig 8A), which is unsurprising given that gB and PC are key targets of CMV-neutralizing antibodies [24,25]. Additionally, principal component analysis (PCA) suggested a clustering of AF-positive separately from AF-negative dams, largely driven by the loading for maternal plasma VL, which was negatively correlated with humoral responses (Fig 8B). However, there is a clear influence of group status, as all of the CD4-depleted dams clustered together (Fig 8C).

Discussion

Despite the high risk setting of primary maternal HCMV infection during pregnancy, only a minority (30–40%) of these cases will congenitally transmit the virus to their fetus. The

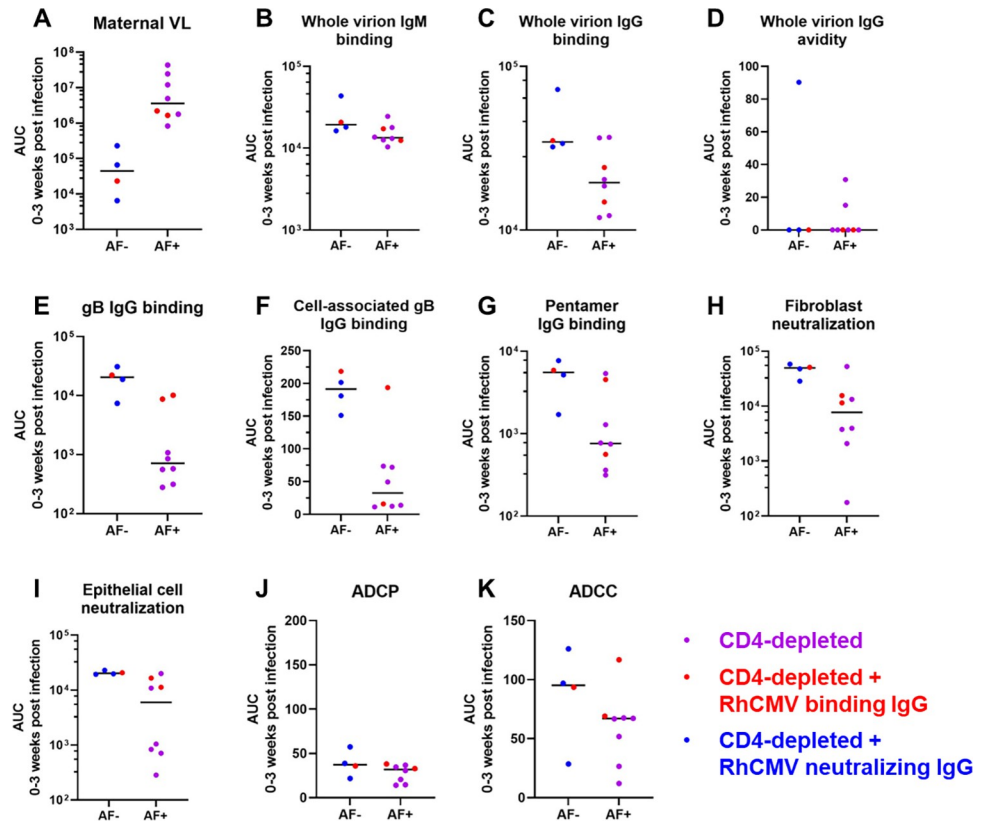


Fig 7. Univariate comparison of maternal VL and humoral responses by vertical transmission status in CD4-depleted dams. The area-under-the-curve (AUC) of each response over 0–3 weeks post RhCMV infection was used to distill the magnitude and kinetics of each response into a single value in a critical window for vertical transmission. Amniotic fluid (AF) was assessed for RhCMV DNA by qPCR and a positive result (AF-positive) was defined by 2 or more of 12 replicates with detectable amplification between 2 and 12 weeks after maternal infection. Pairwise comparisons between AF-positive and AF-negative dams were performed using Wilcoxon Rank Sum Tests (Table 1). VL: viral load; ADCP: antibody dependent cellular phagocytosis; ADCC: antibody dependent cellular cytotoxicity.

<https://doi.org/10.1371/journal.ppat.1011378.g007>

determinants of cCMV transmission following acute maternal CMV infection remain largely unknown yet could be an important guide to effective vaccine development. Human studies have previously suggested that high maternal anti-CMV ADCP responses is associated with protection from vertical HCMV transmission [26]. Yet, human studies are inherently limited by the inability to accurately time primary HCMV infection given its often mild or silent presentation. Furthermore, current guidance limits amniocentesis for diagnosis of cCMV to later than 21 weeks gestation and more than 6 weeks after suspected maternal infection, which may miss early transmission events [27,28]. Thus, the rhesus macaque model of cCMV transmission following acute RhCMV infection in pregnancy represents a unique opportunity to define the early kinetics of virus replication and immunity, as well as their impact on vertical transmission risk.

Importantly, the rhesus macaque model of cCMV transmission following primary RhCMV infection at the end of 1st trimester in immunocompetent dams and utilizing the end point of virus detected in AF between 2 and 12 weeks after infection accurately modeled the epidemiology of human CMV transmission following acute infection during pregnancy, with 5 of 12 dams (41.7%) with virus detection in AF [3]. Yet, contrary to our expectations and challenging a common hypothesis in the field [17,29], we found that maternal plasma VL magnitude and

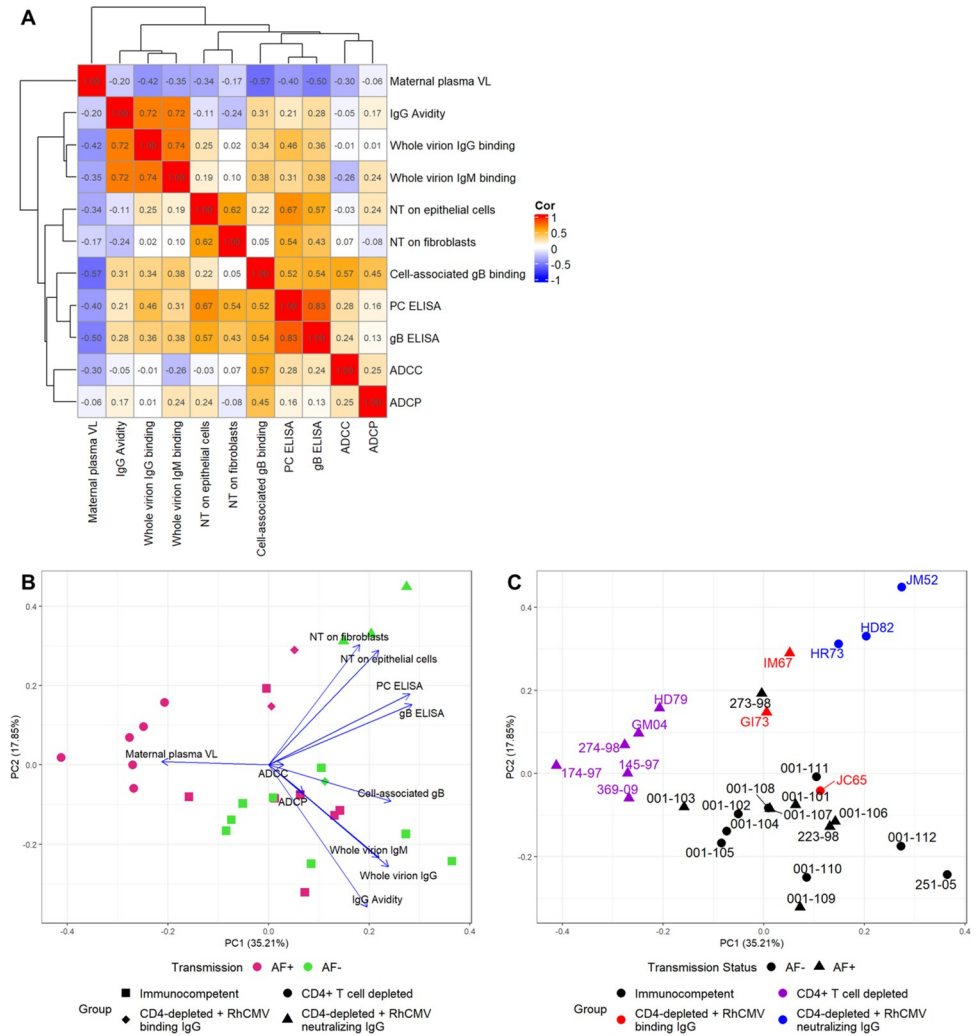


Fig 8. RhCMV-specific antibody responses negatively associate with maternal VL. (A) Correlation matrix showing Spearman correlation coefficients for pairwise correlations between the AUC of each RhCMV-specific antibody response over the first 3 weeks post infection. (B) Principal component analysis (PCA) using the AUC of each response over the first 3 weeks post infection, showing clustering by AF-negative (magenta) versus AF-positive (green) with treatment groups represented by the symbol shape. Loading vectors for each measured response demonstrate the influence of each response. (C) The same PCA with group represented by color, transmission status represented by shape, and animal IDs labeled to better demonstrate the effect of treatment group. VL: viral load; NT: neutralization; PC: pentameric complex; ELISA: enzyme-linked immunosorbent assay; ADPC: antibody dependent cellular phagocytosis; ADCC: antibody dependent cellular cytotoxicity.

<https://doi.org/10.1371/journal.ppat.1011378.g008>

kinetics were not significantly different between AF-positive and AF-negative immunocompetent dams. While the exact mechanism of transplacental CMV transmission has not been fully defined, the notion that more virus circulating in maternal blood leads to greater risk of transmission due to the increased interaction of CMV with the maternal-fetal interface is not supported by these results. Yet, there was a notable difference in the plasma VL of vertically transmitting and non-transmitting dams in the setting of extreme immune suppression via CD4+ T cell depletion. Notably, the VLs of the immunocompetent animals tended to fall in the middle of the overall distribution, and we speculate that the level of maternal viremia may not be a useful predictor of vertical transmission based on this result. However, controlling maternal viremia to a lower level, as we saw in some animals treated with a polyclonal CMV-

targeting IgG infusion, is likely still a worthwhile goal towards the prevention of cCMV. Furthermore, we inoculated these monkeys via intravenous injection with the express purpose of modeling maternal viremia, but oral inoculation, which better models natural routes of infection may yield greater variation in VL in immunocompetent animals [30]. Our findings may provide insight as to why randomized trials of CMV hyperimmune globulin yielded mixed results in reducing cCMV transmission and did not show efficacy in randomized control trials, indicating that post-exposure prophylaxis strategies will have limited efficacy due to a small window of opportunity to prevent vertical transmission in the setting of primary maternal infection [31,32,33]. Yet, this finding does not diminish the potential impact of vaccine-elicited immunity prior to child-bearing years that could reduce the risk of maternal infection and/or congenital transmission.

Also contrary to our expectations, we found no statistically significant differences in humoral immune responses in immunocompetent dams who did and did not have virus detected in AF. We speculate that because transmission often occurs shortly following infection in this setting of primary maternal infection (Fig 5L), the humoral response develops too slowly to protect from vertical transmission. Human studies that have indicated distinct responses are related to transmission status have the advantage of being larger and thus have more statistical power, yet these are complicated by the limited ability to time the infection. The results from this model indicate any differences in humoral responses to acute infection when accurately timed may be very small. Other characteristics of the maternal immune landscape, potentially related to innate immunity or T cell responses, may play more of a role in determining vertical CMV transmission in the context of acute, primary infection. However, as demonstrated by the CD4-depleted dams, pre-existing virus-specific IgG antibodies can protect from vertical RhCMV transmission [16], suggesting that immunization or pre-exposure prophylactic immunotherapeutic strategies are likely to be the most protective approach.

In combining the primarily infected rhesus macaque dams for enhanced variability of antibody levels and power to detect differences in transmitting and non-transmitting dams, only maternal plasma RhCMV gB and PC glycoprotein-specific binding IgG responses were higher magnitude in those dams that did not have virus detected in AF compared to those that did. Interestingly, the cell-associated gB-binding IgG response was statistically different between the groups, but not against soluble gB, paralleling our previous finding that this response was an immune correlate of protection against virus acquisition in gB/MF59 vaccine studies [34]. However, these differences are largely driven by the CD4-depleted groups, as similar trends are observed when we look exclusively at the CD4-depleted groups but are not present in the immunocompetent group. Neutralizing antibodies also stand out as higher magnitude in AF-negative compared to AF-positive dams when focused on the CD4-depleted groups, which is unsurprising given the correlations between gB- and PC-binding IgG and neutralization responses. Furthermore, in the CD4-depleted group, dams receiving potent RhCMV-neutralizing IgG infusion produced from RhCMV-seropositive plasma donors screened for high epithelial cell neutralization were all AF-negative [16]. Thus, the high titers of RhCMV-neutralizing antibodies in this AF-negative cohort compared to that of the other dam groups are expected. In contrast, the RhCMV-specific IgG infusions did not confer high titers of antibodies capable of mediating ADCP and ADCC functions when compared to late timepoints in acutely infected dams, which may be a result of low levels of these types of antibodies in chronically infected animals from whom the IgG for these infusions was purified. Thus, while neutralizing responses were the only functional responses distinct between the CD4-depleted AF-positive and AF-negative dams, these findings may be a result of the experimental design and does not eliminate Fc mediated effector functions as potentially protective IgG responses.

Of note, amniotic fluid VL was detected late (≥ 6 weeks post infection) in two immunocompetent, AF-positive dams. Because AF VL kinetics tend to occur in short blips [15,16], it is possible that these fetuses were infected earlier in gestation and prior AF sampling missed the initial infection. However, these late detection events raise the possibility that the timing of fetal infection may point to different mechanisms of vertical transmission and consequently differences in protective maternal immunity. Given these small numbers in the late versus early AF-positive categories, we cannot perform additional statistical analysis to disentangle any potential interactions of humoral response and timing of detecting fetal infection, but visualizing the antibody kinetics comparing early and late detection of AF-positivity do not demonstrate clear differences (S1 Fig).

A key caveat of this work, and most non-human primate studies, is limited group sizes. Thus, we included dams from prior studies of primary maternal infection in the rhesus macaque model to increase our sample size. This strategy has the advantage for this study of including animals with perturbations to their humoral responses, as CD4+ T cell depletion results in a delay in humoral responses and passive antibody infusion introduces a high titer of RhCMV-specific antibodies prior to infection [15,16]. These prior studies demonstrated that pre-existing antibodies can protect against vertical RhCMV transmission in the high risk setting of CD4-depletion [16]. However, a caveat of including dams from multiple treatment groups is a potential confounding factor since all 3 of the dams receiving the high RhCMV-neutralizing IgG infusion were AF-negative and all 6 of the CD4-depleted dams without IgG infusion were AF-positive. Thus, this analysis is largely exploratory, and further experimentation of critical components of pre-existing immunity and cCMV transmission status would be necessary to confirm the trends observed.

Beyond small sample sizes, we must additionally qualify our conclusions based on the limitations of the animal model. Barring human challenge studies, which would be immensely unethical in the context of pregnancy and fetal infection, rhesus macaque infection with RhCMV is the most translatable model system available to study cCMV [8,11,35]. However, while there is much cross-reactivity between rhesus and human antibodies and Fc receptors (FcRs), there are key immunologic differences in the IgG subclasses that dominantly mediate effector functions, the number of FcR allotypes expressed in each species, and the affinity of antibody-FcR binding interactions [36,37,38,39,40]. Additionally, RhCMV contains most of the same gene families as HCMV and significant functional homology has been observed between the two viruses supporting the use of this model system, but there is little sequence homology, highlighting potential impactful differences between HCMV and RhCMV and their respective hosts [35,41]. Lastly, non-human primates are an excellent model for human placentation compared to other traditional animal models, like rodents, but there are some differences in the structure and development of the placenta between humans and rhesus macaques that could lead to differences in mechanisms of placental CMV transmission [42,43].

While it is promising that we observed a similar rate of vertical CMV transmission in seronegative immunocompetent rhesus dams as has been observed in humans [3], the humoral and virological factors we investigated were largely not associated with AF status. Our findings underscore the need for further research to deconvolute the immune responses necessary for prevention of cCMV infection and ultimately to define targetable factors for vaccines or therapeutics. In the immunocompromised dams, we found that pre-existing antibodies can protect against vertical CMV transmission, suggesting that vaccination to elicit pre-existing IgG responses could be beneficial in prevention of cCMV in seronegative women. Innate immunity, T cell responses, and maternal-fetal interface immunity and inflammation are additional factors that may influence vertical CMV transmission risk [44]. Notably, CMV is also

exceptionally adept at immune evasion as a large portion of its ~235 kilobase genome is devoted to genes with immune evasion functions [45], so countering key immune evasins may additionally be a strategy for improving upon current preventive and therapeutic interventions. These results from our NHP model suggest that natural humoral responses to primary infection during pregnancy will likely not be protective against cCMV infection, so developing effective strategies for establishing robust adaptive immunity prior to pregnancy is paramount to reducing the global burden of CMV-associated birth defects.

Methods

Ethics statement for in vivo non-human primate studies

In vivo non-human primate studies were performed at the Tulane National Primate Research Center (TNPRC) and previously at the New England Primate Research Center (NEPRC). Current and previous studies were carried out in accordance with the Guide for the Care and Use of Laboratory Animals of the NIH [46]. The animal protocol was reviewed and approved by the Institutional Animal Care and Use Committees (IACUCs) at TNPRC and NEPRC. The facilities also maintained an Animal Welfare Assurance statement with the National Institutes of Health, Office of Laboratory Animal Welfare.

Animals

Indian-origin rhesus macaques were from a RhCMV-seronegative expanded specific pathogen-free (eSPF) colony housed at the TNPRC or previously at the NEPRC and maintained in accordance with institutional and federal guidelines for the care and use of laboratory animals [46]. We screened females for RhCMV-specific IgM and IgG via a whole virion ELISA to confirm that they were RhCMV-seronegative. These females, all between 4 and 9 years of age, were co-housed with RhCMV-seronegative males and screened for pregnancy every three weeks via abdominal ultrasound. Sonography was further used to approximate gestational date using the gestational sac size and crown-rump length of the fetus. A total of 27 RhCMV-seronegative dams across past and current studies were inoculated intravenously with RhCMV in late first/early second trimester at approximately 7–9 weeks gestation (Fig 4). Fourteen dams received 1×10^6 pfu each of RhCMV UCD52, UCD59 (previously reported as 1×10^6 TCID₅₀ rounded from 1.4×10^6 TCID₅₀) and 2×10^6 TCID₅₀ of RhCMV 180.92 while one dam received only 2×10^6 TCID₅₀ of RhCMV 180.92 [15,16]. Twelve dams in the current study received 1×10^6 pfu each of RhCMV UCD52 and FL-RhCMV (Fig 4). One week prior to infection, 12 of the dams received 50 mg/kg recombinant rhesus CD4+ T cell-depleting antibody (CD4R1 clone; NIH Nonhuman Primate Reagent Resource) via intravenous infusion [15]. Of the dams receiving the CD4-depletion antibody, 6 also received passive infusion of IgG purified from RhCMV seropositive animals. Three of these received a single infusion 1 hour before inoculation of 100mg/kg of IgG purified from animals screened for high RhCMV-binding via whole virion ELISA. The other three received a dose-optimized regimen of one infusion 1 hour prior to infection of 150 mg/kg and another at 3 days post infection of 100 mg/kg of IgG purified from animals screened for high RhCMV neutralization on epithelial cells [16]. Blood was collected at least one timepoint before administration of any treatments, at the time of CD4+ T cell depletion, at the time of passive antibody infusions, and at the time of infection. The animals receiving passive antibody infusion were additionally sampled at 7–8 hours, 2 days and 4 days post infection. Dams in the new immunocompetent cohort were sampled at days 1 and 4 post infection in the first week. Otherwise, samples were collected on an approximately weekly basis in all groups. Amniocentesis was performed on a weekly to bi-weekly basis, when

possible to perform safely by veterinary staff, until fetal loss ($n = 5$) or until hysterotomy in near-term of pregnancy (gestational weeks 19–22).

Cell culture

Telomerized rhesus fibroblasts (TeloRFs, Barry Lab) [47] were maintained in Dulbecco's modified Eagle medium (DMEM, Gibco) containing 10% heat-inactivated fetal bovine serum (FBS, Corning), 25 mM N-2-hydroxyethylpiperazine-N'-2-ethanesulfonic acid (HEPES, Gibco), 2 mM L-glutamine (Gibco), 50 U/mL penicillin and 50 μ g/mL streptomycin (Gibco), 50 μ g/mL gentamicin (Gibco), and 100 μ g/mL geneticin G418 (Gibco). Monkey kidney epithelial (MKE, Barry Lab) cells were cultured in DMEM-F12 (Gibco) supplemented with 10% FBS, 25 mM HEPES, 2 mM L-glutamine, 1 mM sodium pyruvate (Gibco), 50 U/ml penicillin and 50 μ g/ml streptomycin, and 50 μ g/ml gentamicin. Primary embryonal rhesus fibroblasts (1RFs) were generated at the Oregon National Primate Research Center (ONPRC) and maintained in DMEM supplemented with 10% fetal bovine serum and antibiotics (1 \times Pen/Strep, Gibco), and grown at 37°C in humidified air with 5% CO₂. Human embryonic kidney 293T cells (ATCC) used for transfection were maintained in DMEM supplemented with 10% FBS, 25 mM HEPES, 50 U/mL penicillin and 50 μ g/mL streptomycin. Human monocyte THP-1 cells (ATCC) were maintained in RPMI 1640 medium (Gibco) supplemented with 10% FBS. Human NK92 cells transduced to express the Ile¹⁵⁸ variant of rhesus macaque CD16 (NK92. rh.158I.Bb11, Pollara Lab) were cultured in Myelocult H5100 (STEMCELL) medium supplemented with 10mM HEPES, 1 mM sodium pyruvate, 50 U/ml penicillin and 50 μ g/ml streptomycin, and 50 U/mL recombinant human IL-2 (PeproTech) [33]. Cell lines were generally passaged twice weekly and tested for mycoplasma contamination every 6 months.

Virus growth

Stocks of epithelial-tropic UCD52 was produced by propagating from a seed stock on MKE cells for 2–4 passages and then once of TeloRFs to boost viral titer. Infection was performed in a low volume of 5% FBS medium for at least 2 hours at 37°C and 5% CO₂, a maintenance volume of media was added, and cells were incubated for up to 2 weeks. Virus was harvested when 90% cytopathic effect (CPE) was observed. Cells were collected by scraping and combined with the culture supernatant. Cells were pelleted by low-speed centrifugation and supernatant collected and placed on ice. Cell pellets were resuspended in infection media and combined, then subjected to either three freeze/thaw cycles or sonication. Large cell debris was pelleted by low-speed centrifugation. The supernatants were combined, passed through a 0.45- μ m filter, overlaid onto a 20% sucrose cushion, and then ultracentrifuged at 70,000 \times g for 2 hours at 4°C using an SW28 Beckman Coulter rotor. Virus pellets were resuspended in DMEM containing 10% sucrose, aliquoted and stored at -80°C until final use. All viruses were titered on TeloRFs and/or MKE cells (depending on the intended use) using the TCID₅₀ method, staining cells infected with a serial dilution (covering 10³–10⁸-fold with 8–24 replicates of each dilution) of the concentrated virus stock for RhCMV IE-1 or Rh152/151 (primary antibodies provided by OHSU) in black, clear bottom 96-well flat bottom plates (Corning).

FL-RhCMV is a previously described fully repaired version of the laboratory RhCMV strain 68–1 [13]. FL-RhCMV was reconstituted in 1RFs by transfecting purified BAC DNA using Lipofectamine 3000 (Thermo Fisher Scientific). 1RFs were passaged weekly until full CPE were observed. Cells and supernatants of one T-175 flask were harvested and used to infect 8 \times T-175 flasks containing a confluent monolayer of 1RFs to produce a high titer stock. Cells and supernatants were harvested at maximal CPE and stored together over night at -80°C to release virus from the infected cells. The cellular supernatants were subsequently clarified by

centrifugation at $7,500 \times g$ for 15 min and the clarified culture medium was layered over a sorbitol cushion (20% d-sorbitol, 50 mM Tris [pH 7.4], 1 mM $MgCl_2$). FL-RhCMV was pelleted by centrifugation at 22,000 rpm for 1 hour at $4^\circ C$ in a Beckman SW28 rotor and the resulting virus pellet was resuspended in DMEM, aliquoted and stored at $-80^\circ C$ until final use.

Viral load

RhCMV DNA was quantified in maternal plasma and fetal amniotic fluid via qPCR. DNA was isolated from the amniotic fluid by using the QIAmp DNA minikit (Qiagen). We utilized either a 45-cycle real-time qPCR reaction using 5'-GTTTAGGGAACCGCCATTCTG-3' forward primer, 5'-GTATCCGCGTTCCAATGCA-3' reverse primer, and 5'-FAM-TCCAGCC TCCATAGCCGGGAAGG-TAMRA-3' probe directed against a 108bp region of the highly conserved noncoding exon 1 of the RhCMV IE gene [20], or a 40-cycle reaction using 5'-TGCGTACTATGGAAGAGACAATGC-3' forward primer, 5'-ACATCTGGCCGTTCAA AAAAAC-3' reverse primer, and 5'-TET-CCAGAAGTTGCGCATCCGCTTGT-TAMRA-3' probe against the gB gene (*UL55* accession no. U41526) [48]. Each assay used a standard IE or gB amplicon plasmid to interpolate the number of viral DNA copies/mL of plasma or amniotic fluid. These two assays were validated against one another to ensure consistent results. Vertical transmission was defined as 2 or more of 12 technical replicates above the limit of detection (1–10 copies per reaction) for each amniotic fluid sample. Two out of six replicates above the limit of detection was required to report a positive result for each plasma sample.

Serology assays

RhCMV-specific IgG binding and avidity kinetics were measured in plasma by enzyme-linked immunosorbent assays (ELISAs) using either whole-virion preparations of RhCMV strain UCD52 or purified glycoprotein preparations of gB or PC as described previously [16]. Briefly, high-binding 384-well ELISA plates (Corning) were coated with 15 μL /well of antigen overnight at $4^\circ C$. For whole virion ELISAs, filtered RhCMV UCD52 was diluted to 5,120 pfu/mL in phosphate buffered saline (PBS) with Mg^{2+} and Ca^{2+} for coating, while soluble glycoprotein preparations were coated at 2 $\mu g/mL$ in 0.1M sodium bicarbonate. Following overnight incubation, plates were washed using an automated plate washer (BioTek) and blocked for 2 hours with blocking solution (PBS+, 4% whey protein, 15% goat serum, 0.5% Tween-20), and then 3-fold serial dilutions of plasma (1:30 to 1:65,610) were added to the wells in duplicate for 1.5 hours. For avidity assays, plates were washed once, and 20 μL per well of PBS or 7M urea was added to the wells for 6 minutes. Plates were then washed once and incubated for 1 hour with mouse anti-monkey IgG HRP-conjugated secondary antibody (Southern Biotech, clone SB108a, cat. # 4700–05) at a 1:5,000 dilution or goat anti-monkey IgM HRP-conjugated secondary antibody (Rockland, cat. #617-101-007) at 1:8,000. After two washes, SureBlue Reserve TMB Microwell Peroxidase Substrate (KPL) was added to the wells for 7 minutes for whole virion ELISAs and 3.5 minutes for glycoprotein ELISAs, and the reaction was stopped by addition of 1% HCl solution (KPL). Plates were read at 450 nm (OD_{450}) and reported as median effective dilution factor (ED_{50}) for purified protein ELISAs. AUC of the OD_{450} values over the dilution series was reported for the whole virion ELISAs as these resulted in incomplete sigmoidal curves and thus would not yield reliable ED_{50} calculations (S2 Fig). The lower threshold for antibody reactivity was considered to be 3 standard deviations above the average OD_{450} measured for RhCMV-seronegative samples at the starting plasma dilution (1:30). ED_{50} was calculated as the sample dilution where 50% binding occurs by interpolation of the sigmoidal binding curve using four-parameter logistic regression, and this value was set to half of

the starting dilution [15] when the 1:30 dilution point was negative by our cutoff and when the calculated ED₅₀ was below 15.

Neutralization of RhCMV on fibroblasts and epithelial cells was monitored as previously described [16]. Briefly, serial dilutions (1:10 to 1:30,000 or 1:30 to 1:65,610) of heat-inactivated rhesus plasma were incubated with FL-RhCMV [19] or RhCMV UCD52 (MOI = 1) for 1–2 hours at 37°C. The virus/plasma dilutions were then added in duplicate to 384-well plates containing confluent cultures of TeloRF or MKE cells, respectively, and incubated at 37°C for 24 or 48 hours, respectively. Infected cells were then fixed for 20 minutes in 10% formalin and processed for immunofluorescence with 1 µg/mL mouse anti-RhCMV pp65B or 5 µg/mL mouse anti-Rh152/151 monoclonal antibody (both produced from hybridoma lines generated at OHSU) followed by a 1:500 dilution of goat anti-mouse IgG-Alexa Fluor 488 antibody (Invitrogen, cat. # A28175). Nuclei were stained with 4',6-diamidino-2-phenylindole (DAPI, Invitrogen) for 10 minutes. Infection was quantified in each well by automated cell counting software using one of the following instruments at 10X magnification: (a) a Nikon Eclipse TE2000-E fluorescence microscope equipped with a CoolSNAP HQ-2 camera, (b) a Cellomics CX5 or Arrayscan VTI HCS instrument, or (c) a Molecular Devices ImageXpress Pico. Subsequently, the 50% inhibitory dilution factor (ID₅₀) was calculated as the sample dilution that caused a 50% reduction in the number of infected cells compared with wells treated with virus only. If the ID₅₀ was below the limit of detection (e.g., every value in the series resulted in a high level of infection above 50%), we set the ID₅₀ to half of the first dilution. Similarly, for samples above the upper limit of detection (e.g., all points in the series resulted in levels of infection below 50%), we set the ID₅₀ at the value of the last dilution point.

Cell-associated gB binding was measured using a gB-transfected-cell binding assay [34]. 293T cells at 50–80% confluence were co-transfected with 1 µg of each GFP (Ampicillin-resistant pGAE-CMV-GFP-WPRE, gift of M. Blasi, Duke University) and UCD52 gB (Ampicillin-resistant pcDNA3.1+ vector) using the Effectene transfection kit (Qiagen) and incubated for 48 hours. Following transfection, GFP expression was confirmed using a fluorescent microscope prior to harvest. Cells were then dissociated from culture flasks using TrypLE (Gibco), and 100,000 cells per well were added to 96-well V-bottom plates (Corning). Transfected cells were incubated with plasma samples at a 1:600 dilution in duplicate for 2 h. Cells were then washed and resuspended in far red live/dead stain (Invitrogen) at 1:1000 and incubated for 20 minutes. Following another wash, cells were resuspended in 1:200 of anti-monkey IgG-PE (Southern Biotech, clone SB108a, cat. # 4700–09) for 25 minutes at RT. Cells were then washed twice and fixed for 20 minutes in 10% formalin and resuspended in PBS. Fluorescence was measured using a BD LSRII or Fortessa flow cytometer, and data is reported as the percent of the live population that is GFP and PE double positive.

Antibody-dependent cellular phagocytosis was assessed by conjugation of concentrated RhCMV UCD52 to Alexa Fluor 647 using NHS-ester reaction (Invitrogen), which was allowed to proceed in the dark with constant agitation for 1–2 hours. The reaction was quenched by the addition of pH 8.0 Tris-HCl, and the conjugated virus was diluted to 7x10⁶ pfu/mL. Equal amounts (10 µL) of virus and plasma samples in duplicate at a 1:30 dilution were combined in a 96-well U-bottom plate (Corning) and incubated at 37°C for 2 hours. THP-1 monocytes were then added at 50,000 cells per well. Plates were spun for 1 hour at 1200 x g at 4°C in a spinoculation step and then transferred to a 37°C incubator for an additional 1 hour. Cells were then washed and stained with aqua live/dead (Invitrogen) at 1:1000 for 20 minutes. Following another wash step, cells were fixed for 20 minutes in 10% formalin and resuspended in PBS. Fluorescence was measured using a BD LSRII or Fortessa flow cytometer, and data is reported as the percent of the live population that was AF647+, with the threshold for AF647-positivity was set based on no antibody control wells. Known RhCMV-seronegative plasma samples

served as negative controls, and known seropositive plasma samples and purified IgG from seropositive animals served as positive controls in each assay.

Antibody-dependent cellular cytotoxicity was measured by NK cell degranulation using NK92.rh.158I.Bb11, an engineered NK cell line expressing the Ile¹⁵⁸ variant of rhesus macaque CD16 [49]. Confluent TeloRF cells were infected with 1 MOI UCD52 RhCMV in low serum (5%) medium in T75 flasks (ThermoFisher). Mock infection was performed in parallel. After 24 hours of infection, cells were dissociated from the flask using TrypLE (Gibco), and 50,000 target cells were seeded in each well of a 96-well flat bottom tissue culture plate (Corning). Cells were incubated for 16–20 hours to allow them to adhere. Then, the target cell medium was removed, and to each well, 50,000 NK92.Rh.CD16-Bb11 cells were added with plasma samples at 1:25 dilution or purified IgG from either seropositive or seronegative plasma donors at 50–250 µg/mL in R10 (RPMI1640 containing 10% FBS), plated in duplicate. The same samples were added to mock-infected target cells for background subtraction. Brefeldin A (GolgiPlug, 1:1000, BD Biosciences), monensin (GolgiStop, 1:1500, BD Biosciences), and mouse anti-human CD107a-FITC (BD Biosciences, 1:40, clone H4A3, cat. # 555800) were added to each well for a total of 100µL and co-incubated for 6 hours at 37°C and 5% CO₂. NK cells were then collected and transferred to a 96-well V-bottom plate (Corning). Cells were pelleted, washed with PBS, and then resuspended in aqua live/dead diluted 1:1000 for a 20-minute incubation at RT. Cells were washed with PBS + 1% FBS and stained with mouse anti-human CD56-PECy7 (BD Biosciences, clone NCAM16.2, cat. # 557747) and mouse anti-human CD16 PacBlue (BD Biosciences, clone 3G8, cat. #558122) for a 20-minute incubation at RT. Cells were washed twice then resuspended in 10% formalin fixative for 20 minutes or 1% formalin overnight. Cells were then resuspended in PBS for acquisition. Events were acquired on a BD Symphony A5 using the high-throughput sampler (HTS) attachment, and data analysis was performed using FlowJo software (v10.8.1). Data is reported as the background-subtracted % of CD107a+ live NK cells (singlets, lymphocytes, aqua blue-, CD56+, CD107a+) for each sample. Each assay included purified IgG from RhCMV-seropositive and -seronegative macaques as positive and negative controls, respectively.

Statistical analysis

For each biomarker we calculated the area under the curve from day 0 to day 21. In instances where there was not a day 0 value, we either A) carried forward the last value before infection (if existed) or B) linearly back-extrapolated from the first two values after infection. When there were no day 21 values, we either A) linearly extrapolated between last value before day 21 and first value after day 21 (if existed) or B) carried forward last value before day 21 (if no value post day 21). We performed exact Wilcoxon-rank sum tests using the coin package in R [50]. Multiple testing correction was done using Benjamini-Hochberg FDR method with significance deemed as an adjusted p-value less than 0.2 and an unadjusted less than 0.05 [51]. In the combined analyses, we used the coin package again but performed the analysis stratified by immune status (this assumes similar association across groups). PCA was calculated in R using prcomp.

Supporting information

S1 Fig. Response kinetics in immunocompetent dams with early (≤ 4 weeks post infection, grey) versus late (≥ 6 weeks post infection, green) detection of RhCMV in amniotic fluid. (A) Maternal plasma VL measured by qPCR for the UL55 or IE genes; (B) IgM and (C) IgG binding to whole UCD52 RhCMV virions; (D) avidity of IgG binding against whole UCD52 virions; IgG binding to (E) PC, (F) soluble gB ectodomain by ELISA, and (G) cell-associated

gB via transfected cell binding assay; antibody mediated RhCMV neutralization on (H) fibroblasts and (I) epithelial cells; (J) ADCP; and (K) ADCC.

(TIF)

S2 Fig. Representative ELISA results. The optical density at 450 nm (OD_{450}) are plotted versus log dilution factor for (A) whole virion IgM binding, (B) whole virion IgG binding, (C) gB IgG binding, and (D) PC IgG binding. One animal from each treatment group is represented, showing the samples taken at the time of infection and 21- or 28-days post infection.

(TIF)

Acknowledgments

The authors would first like to acknowledge the rhesus macaques that were used in this study and thank the faculty and staff of the Departments of Veterinary Medicine and Collaborative Research at the Tulane National Primate Research Center (TNPRC) for their excellent care of our research animals. We would like to thank former lab staff, namely Kristy Bialas and Eduardo Cisneros de la Rosa, for the contribution of previously published ELISA and neutralization data included in this analysis. We acknowledge the Molecular Virology Core at Oregon National Primate Research Center (ONPRC) for performing viral productions. We are additionally grateful to the NIH Nonhuman Primate Reagent Resource (R24 OD010976 and NIAID contract HHSN 272201300031C) which provided the CD4-depleting antibody used in the historical studies. We further wish to acknowledge support from the Biostatistics, Epidemiology and Research Design (BERD) Methods Core.

Author Contributions

Conceptualization: Claire E. Otero, Peter A. Barry, Amitinder Kaur, Sallie R. Permar.

Data curation: Claire E. Otero, Richard Barfield, Elizabeth Scheef, Cody S. Nelson, Nicole Rodgers, Hsuan-Yuan Wang, Matilda J. Moström, Julian Sass, Angel Davalos.

Formal analysis: Richard Barfield, Julian Sass, Cliburn Chan.

Funding acquisition: Peter A. Barry, Klaus Früh, Amitinder Kaur, Sallie R. Permar.

Investigation: Claire E. Otero, Elizabeth Scheef, Cody S. Nelson, Nicole Rodgers, Hsuan-Yuan Wang, Matilda J. Moström, Tabitha D. Manuel, Julian Sass, Kimberli Schmidt, Husam Taher, Courtney Papen, Lesli Sprehe, Savannah Kendall, Daniel Malouli.

Methodology: Claire E. Otero, Justin Pollara, Daniel Malouli.

Resources: Husam Taher, Courtney Papen, Klaus Früh, Daniel Malouli.

Supervision: Peter A. Barry, Klaus Früh, Justin Pollara, Daniel Malouli, Cliburn Chan, Amitinder Kaur, Sallie R. Permar.

Validation: Claire E. Otero, Richard Barfield, Hsuan-Yuan Wang, Angel Davalos, Cliburn Chan.

Visualization: Claire E. Otero, Richard Barfield, Julian Sass.

Writing – original draft: Claire E. Otero.

Writing – review & editing: Richard Barfield, Cody S. Nelson, Matilda J. Moström, Husam Taher, Angel Davalos, Justin Pollara, Daniel Malouli, Cliburn Chan, Amitinder Kaur, Sallie R. Permar.

References

1. Goderis J, De Leenheer E, Smets K, Van Hoecke H, Keymeulen A, Dhooge I. Hearing loss and congenital CMV infection: a systematic review. *Pediatrics*. 2014; 134(5):972–82. <https://doi.org/10.1542/peds.2014-1173> PMID: 25349318
2. Kenneson A, Cannon MJ. Review and meta-analysis of the epidemiology of congenital cytomegalovirus (CMV) infection. *Rev Med Virol*. 2007; 17(4):253–76. <https://doi.org/10.1002/rmv.535> PMID: 17579921
3. Simonazzi G, Curti A, Cervi F, Gabrielli L, Contoli M, Capretti MG, et al. Perinatal Outcomes of Non-Primary Maternal Cytomegalovirus Infection: A 15-Year Experience. *Fetal Diagn Ther*. 2018; 43(2):138–42. <https://doi.org/10.1159/000477168> PMID: 28697499
4. Zuhair M, Smit GSA, Wallis G, Jabbar F, Smith C, Devleeschauwer B, et al. Estimation of the worldwide seroprevalence of cytomegalovirus: A systematic review and meta-analysis. *Rev Med Virol*. 2019; 29(3):e2034. <https://doi.org/10.1002/rmv.2034> PMID: 30706584
5. McGeoch DJ, Cook S, Dolan A, Jamieson FE, Telford EA. Molecular phylogeny and evolutionary time-scale for the family of mammalian herpesviruses. *J Mol Biol*. 1995; 247(3):443–58. <https://doi.org/10.1006/jmbi.1995.0152> PMID: 7714900
6. Marsh AK, Ambagala AP, Perciani CT, Russell JN, Chan JK, Janes M, et al. Examining the species-specificity of rhesus macaque cytomegalovirus (RhCMV) in cynomolgus macaques. *PLoS One*. 2015; 10(3):e0121339. <https://doi.org/10.1371/journal.pone.0121339> PMID: 25822981
7. Weisblum Y, Panet A, Haimov-Kochman R, Wolf DG. Models of vertical cytomegalovirus (CMV) transmission and pathogenesis. *Semin Immunopathol*. 2014; 36(6):615–25. <https://doi.org/10.1007/s00281-014-0449-1> PMID: 25291972
8. Roark HK, Jenks JA, Permar SR, Schleiss MR. Animal Models of Congenital Cytomegalovirus Transmission: Implications for Vaccine Development. *J Infect Dis*. 2020; 221(Suppl 1):S60–s73. <https://doi.org/10.1093/infdis/jiz484> PMID: 32134481
9. Haigwood NL WC. Commissioned Paper: Comparison of Immunity to Pathogens in Humans, Chimpanzees, and Macaques. In: Altevogt BM PD, Shelton-Davenport MK, et al., editors., editor. *Chimpanzees in Biomedical and Behavioral Research: Assessing the Necessity*. Washington (DC): National Academies Press (US); 2011.
10. Li M, Brokaw A, Furuta AM, Coler B, Obregon-Perko V, Chahroudi A, et al. Non-human Primate Models to Investigate Mechanisms of Infection-Associated Fetal and Pediatric Injury, Teratogenesis and Stillbirth. *Front Genet*. 2021; 12:680342. <https://doi.org/10.3389/fgene.2021.680342> PMID: 34290739
11. Barry PA, Lockridge KM, Salamat S, Tinling SP, Yue Y, Zhou SS, et al. Nonhuman primate models of intrauterine cytomegalovirus infection. *Ilar j*. 2006; 47(1):49–64. <https://doi.org/10.1093/ilar.47.1.49> PMID: 16391431
12. Itell HL, Kaur A, Deere JD, Barry PA, Permar SR. Rhesus monkeys for a nonhuman primate model of cytomegalovirus infections. *Curr Opin Virol*. 2017; 25:126–33. <https://doi.org/10.1016/j.coviro.2017.08.005> PMID: 28888133
13. Cagliani R, Forni D, Mozzi A, Sironi M. Evolution and Genetic Diversity of Primate Cytomegaloviruses. *Microorganisms*. 2020; 8(5). <https://doi.org/10.3390/microorganisms8050624> PMID: 32344906
14. Frueh KM D; Oxford K; Barry PA. Cytomegaloviruses. In: Reddehase MJ, editor. Volume II2013. p. 463–96.
15. Bialas KM, Tanaka T, Tran D, Varner V, Cisneros De La Rosa E, Chiuppesi F, et al. Maternal CD4+ T cells protect against severe congenital cytomegalovirus disease in a novel nonhuman primate model of placental cytomegalovirus transmission. *Proceedings of the National Academy of Sciences*. 2015; 112(44):13645–50.
16. Nelson CS, Cruz DV, Tran D, Bialas KM, Stamper L, Wu H, et al. Preexisting antibodies can protect against congenital cytomegalovirus infection in monkeys. *JCI Insight*. 2017; 2(13). <https://doi.org/10.1172/jci.insight.94002> PMID: 28679960
17. Gong Y, Moström M, Otero C, Valencia S, Kaur A, Permar SR, et al. Mathematical Modeling of Rhesus Cytomegalovirus (RhCMV) Placental Transmission in Seronegative Rhesus Macaques. *bioRxiv*. 2022:2022.04.07.487583.
18. Jarvis MA, Nelson JA. Human cytomegalovirus persistence and latency in endothelial cells and macrophages. *Curr Opin Microbiol*. 2002; 5(4):403–7. [https://doi.org/10.1016/s1369-5274\(02\)00334-x](https://doi.org/10.1016/s1369-5274(02)00334-x) PMID: 12160860
19. Taher H, Mahyari E, Kreklywich C, Uebelhoer LS, McArdle MR, Moström MJ, et al. In vitro and in vivo characterization of a recombinant rhesus cytomegalovirus containing a complete genome. *PLoS Pathog*. 2020; 16(11):e1008666. <https://doi.org/10.1371/journal.ppat.1008666> PMID: 33232376
20. Kaur A, Hale CL, Noren B, Kassis N, Simon MA, Johnson RP. Decreased frequency of cytomegalovirus (CMV)-specific CD4+ T lymphocytes in simian immunodeficiency virus-infected rhesus macaques:

- inverse relationship with CMV viremia. *J Virol.* 2002; 76(8):3646–58. <https://doi.org/10.1128/jvi.76.8.3646-3658.2002> PMID: 11907204
21. In: Murphy K, editor. *Janeway's Immunobiology.* 8th ed: Garland Science; 2012.
 22. Alter G, Malenfant JM, Altfeld M. CD107a as a functional marker for the identification of natural killer cell activity. *J Immunol Methods.* 2004; 294(1–2):15–22. <https://doi.org/10.1016/j.jim.2004.08.008> PMID: 15604012
 23. Boppana SB, Britt WJ. Antiviral antibody responses and intrauterine transmission after primary maternal cytomegalovirus infection. *J Infect Dis.* 1995; 171(5):1115–21. <https://doi.org/10.1093/infdis/171.5.1115> PMID: 7751685
 24. Reuter N, Kropff B, Britt WJ, Mach M, Thomas M. Neutralizing Antibodies Limit Cell-Associated Spread of Human Cytomegalovirus in Epithelial Cells and Fibroblasts. *Viruses.* 2022; 14(2). <https://doi.org/10.3390/v14020284> PMID: 35215877
 25. Sandoñis V, García-Ríos E, McConnell MJ, Pérez-Romero P. Role of Neutralizing Antibodies in CMV Infection: Implications for New Therapeutic Approaches. *Trends Microbiol.* 2020; 28(11):900–12. <https://doi.org/10.1016/j.tim.2020.04.003> PMID: 32448762
 26. Semmes EC, Miller IG, Wimberly CE, Phan CT, Jenks JA, Harnois MJ, et al. Maternal Fc-mediated non-neutralizing antibody responses correlate with protection against congenital human cytomegalovirus infection. *J Clin Invest.* 2022; 132(16). <https://doi.org/10.1172/JCI156827> PMID: 35763348
 27. Tanimura K, Yamada H. Maternal and neonatal screening methods for congenital cytomegalovirus infection. *J Obstet Gynaecol Res.* 2019; 45(3):514–21. <https://doi.org/10.1111/jog.13889> PMID: 30590863
 28. Yinon Y, Farine D, Yudin MH. Screening, diagnosis, and management of cytomegalovirus infection in pregnancy. *Obstet Gynecol Surv.* 2010; 65(11):736–43. <https://doi.org/10.1097/OGX.0b013e31821102b4> PMID: 21375790
 29. Leruez-Ville M, Sellier Y, Salomon LJ, Stirnemann JJ, Jacquemard F, Ville Y. Prediction of fetal infection in cases with cytomegalovirus immunoglobulin M in the first trimester of pregnancy: a retrospective cohort. *Clin Infect Dis.* 2013; 56(10):1428–35. <https://doi.org/10.1093/cid/cit059> PMID: 23392397
 30. Yue Y, Chang WLW, Li J, Nguyen N, Schmidt KA, Dormitzer PR, et al. Pathogenesis of Wild-Type-Like Rhesus Cytomegalovirus Strains following Oral Exposure of Immune-Competent Rhesus Macaques. *J Virol.* 2022; 96(3):e0165321. <https://doi.org/10.1128/JVI.01653-21> PMID: 34788083
 31. Sebghati M, Khalil A. New evidence on prognostic features, prevention and treatment of congenital Cytomegalovirus infection. *Curr Opin Obstet Gynecol.* 2020; 32(5):342–50. <https://doi.org/10.1097/GCO.0000000000000651> PMID: 32739974
 32. Hughes BL, Clifton RG, Rouse DJ, Saade GR, Dinsmoor MJ, Reddy UM, et al. A Trial of Hyperimmune Globulin to Prevent Congenital Cytomegalovirus Infection. *New England Journal of Medicine.* 2021; 385(5):436–44. <https://doi.org/10.1056/NEJMoa1913569> PMID: 34320288
 33. Kagan KO, Enders M, Schampera MS, Baeumel E, Hoopmann M, Geipel A, et al. Prevention of maternal-fetal transmission of cytomegalovirus after primary maternal infection in the first trimester by biweekly hyperimmunoglobulin administration. *Ultrasound Obstet Gynecol.* 2019; 53(3):383–9.
 34. Jenks JA, Nelson CS, Roark HK, Goodwin ML, Pass RF, Bernstein DI, et al. Antibody binding to native cytomegalovirus glycoprotein B predicts efficacy of the gB/MF59 vaccine in humans. *Sci Transl Med.* 2020; 12(568).
 35. Powers C, Früh K. Rhesus CMV: an emerging animal model for human CMV. *Med Microbiol Immunol.* 2008; 197(2):109–15. <https://doi.org/10.1007/s00430-007-0073-y> PMID: 18193454
 36. Boesch AW, Miles AR, Chan YN, Osei-Owusu NY, Ackerman ME. IgG Fc variant cross-reactivity between human and rhesus macaque FcγRs. *MAbs.* 2017; 9(3):455–65.
 37. Pollara J, Tay MZ, Edwards RW, Goodman D, Crowley AR, Edwards RJ, et al. Functional Homology for Antibody-Dependent Phagocytosis Across Humans and Rhesus Macaques. *Front Immunol.* 2021; 12:678511. <https://doi.org/10.3389/fimmu.2021.678511> PMID: 34093580
 38. Crowley AR, Osei-Owusu NY, Dekkers G, Gao W, Wuhler M, Magnani DM, et al. Biophysical Evaluation of Rhesus Macaque Fc Gamma Receptors Reveals Similar IgG Fc Glycoform Preferences to Human Receptors. *Front Immunol.* 2021; 12:754710. <https://doi.org/10.3389/fimmu.2021.754710> PMID: 34712242
 39. Boesch AW, Osei-Owusu NY, Crowley AR, Chu TH, Chan YN, Weiner JA, et al. Biophysical and Functional Characterization of Rhesus Macaque IgG Subclasses. *Front Immunol.* 2016; 7:589. <https://doi.org/10.3389/fimmu.2016.00589> PMID: 28018355
 40. Chan YN, Boesch AW, Osei-Owusu NY, Emileh A, Crowley AR, Cocklin SL, et al. IgG Binding Characteristics of Rhesus Macaque FcγR. *J Immunol.* 2016; 197(7):2936–47.

41. Pande NT, Powers C, Ahn K, Früh K. Rhesus cytomegalovirus contains functional homologues of US2, US3, US6, and US11. *J Virol*. 2005; 79(9):5786–98. <https://doi.org/10.1128/JVI.79.9.5786-5798.2005> PMID: 15827193
42. Rosenkrantz JL, Gaffney JE, Roberts VHJ, Carbone L, Chavez SL. Transcriptomic analysis of primate placentas and novel rhesus trophoblast cell lines informs investigations of human placentation. *BMC Biol*. 2021; 19(1):127. <https://doi.org/10.1186/s12915-021-01056-7> PMID: 34154587
43. de Rijk EPCT, Van Esch E. The Macaque Placenta—A Mini-Review. *Toxicologic Pathology*. 2008; 36(7_suppl):108S–18S.
44. Itell HL, Nelson CS, Martinez DR, Permar SR. Maternal immune correlates of protection against placental transmission of cytomegalovirus. *Placenta*. 2017; 60 Suppl 1(Suppl 1):S73–s9. <https://doi.org/10.1016/j.placenta.2017.04.011> PMID: 28456432
45. Powers C, DeFilippis V, Malouli D, Früh K. Cytomegalovirus immune evasion. *Curr Top Microbiol Immunol*. 2008; 325:333–59. https://doi.org/10.1007/978-3-540-77349-8_19 PMID: 18637515
46. Council NR. *Guide for the Care and Use of Laboratory Animals: Eighth Edition*. Washington, DC: The National Academies Press; 2011. 246 p.
47. Chang WL, Kirchoff V, Pari GS, Barry PA. Replication of rhesus cytomegalovirus in life-expanded rhesus fibroblasts expressing human telomerase. *J Virol Methods*. 2002; 104(2):135–46. [https://doi.org/10.1016/s0166-0934\(02\)00060-5](https://doi.org/10.1016/s0166-0934(02)00060-5) PMID: 12088823
48. Sequar G, Britt WJ, Lakeman FD, Lockridge KM, Tarara RP, Canfield DR, et al. Experimental coinfection of rhesus macaques with rhesus cytomegalovirus and simian immunodeficiency virus: pathogenesis. *J Virol*. 2002; 76(15):7661–71. <https://doi.org/10.1128/jvi.76.15.7661-7671.2002> PMID: 12097580
49. Tolbert WD, Gohain N, Kremer PG, Hederman AP, Nguyen DN, Van V, et al. Decoding human-macaque interspecies differences in Fc-effector functions: The structural basis for CD16-dependent effector function in Rhesus macaques. *Frontiers in Immunology*. 2022; 13. <https://doi.org/10.3389/fimmu.2022.960411> PMID: 36131913
50. Hothorn T, Hornik K, van de Wiel MA, Zeileis A. Implementing a Class of Permutation Tests: The coin Package. *Journal of Statistical Software*. 2008; 28(8):1–23.
51. Benjamini Y, Hochberg Y. Controlling the False Discovery Rate: A Practical and Powerful Approach to Multiple Testing. *Journal of the Royal Statistical Society Series B (Methodological)*. 1995; 57(1):289–300.